

## **Observation of $\beta$ -Amyloid Peptide Oligomerization by Pressure-Jump NMR Spectroscopy**

C. Ashley Barnes,<sup>§</sup> Angus J. Robertson,<sup>§</sup> John M. Louis, Philip Anfinrud, and Ad Bax\*

Laboratory of Chemical Physics, National Institute of Diabetes and Digestive and Kidney Diseases, National Institutes of Health, Bethesda, MD 20892

**Supporting Information**

## Experimental Methods

### NMR

All NMR and EM experiments were performed in 20 mM KCl, 70 mM potassium phosphate pH 6.0 with 2% D<sub>2</sub>O. Lyophilized peptide was initially dissolved in 180  $\mu$ L 25 mM KOH to which was added a mixture of 18  $\mu$ L 250 mM HCl and 40  $\mu$ L 0.35 M potassium phosphate pH 6.0, immediately prior to loading of the sample into the high-pressure tube.<sup>1</sup> All sample preparation prior to raising the pressure in the NMR sample tube was carried out on ice.

NMR experiments were also carried out in MES buffer, pH 6.3, with the expectation that the oligomer solubilizes more rapidly at high pressure when the pressure raises the sample pH to *ca* 6.8, in contrast to dropping the pressure of pH 6 phosphate buffer to *ca* 5.2.<sup>2</sup> However, overall best results, in particular with respect to the number of pressure cycles before the irreversible formation of pressure-resistant species was obtained in phosphate buffer, and all reported results therefore were recorded in phosphate buffer.

Uniformly <sup>15</sup>N-enriched A $\beta$ <sup>40</sup> peptide samples were obtained as lyophilized powder from either Alexotech (<https://www.alexotech.com>) or prepared in-house following a protocol similar to that used for preparing A $\beta$ <sup>42,3</sup> with the inclusion of a final HPLC purification step.

NMR spectra were recorded using an in-phase refocused heteronuclear gradient-enhanced HSQC pulse sequence, but with a period during which the pressure was dropped to 1 bar inserted immediately after the initial refocused INEPT block (Figure S1), followed by a “melting delay” at high pressure, prior to <sup>15</sup>N evolution. Technical aspects of this pressure switching were described previously,<sup>4</sup> and a 9-second inter-scan delay at high pressure was used for all experiments to allow for complete dissolving of the oligomeric species, and to provide time for the system to re-equilibrate after each full pressure cycle.

Uniformly sampled pressure-jump T<sub>1</sub> spectra were recorded at 600 MHz on a Bruker Avance III system equipped with a z-axis gradient cryogenic probe, using the pulse scheme of Figure S1. The NMR sample contained *ca.* 1.3 mM <sup>15</sup>N labelled A $\beta$ <sub>40</sub>. The spectra were acquired with a 21.9 ppm spectral width in the <sup>15</sup>N dimension and an acquisition time of 75 ms and 14 ppm spectral width and an acquisition time of 120 ms in the <sup>1</sup>H dimension. Spectra for low-pressure delays of 5.5 s and 8 s were acquired in an interleaved manner, with eight scans per FID; a reference spectrum with a low-pressure duration of 200 ms, two scans per FID, was recorded immediately following this acquisition. In the subsequent analysis, spectral intensities were scaled to account for the difference in the number of scans, and the *ca* two-fold lower concentration of monomeric peptide at the start of the reference spectrum.

The pressure-jump T<sub>2</sub> spectra were recorded using the pulse scheme of Figure S2 on a sample, freshly prepared in the same way as above. Spectra with different positions of the Hahn-echo block, T<sub>H</sub>, and with different Hahn-echo delays,  $\kappa$ , were recorded in an interleaved manner such that all FIDs were acquired at comparable concentrations of the gradually pressure-resistant turning sample. Specifically, spectra were generated from sums of 64 FIDs, recorded in the order  $\kappa = \kappa_1, \kappa_2, \kappa_3$ , and repeated for T<sub>H</sub> = 1.25, 2.5, 3.75, 3.75, 2.5, 1.25 s, with the entire set (involving a total of 1152 pressure cycles) recorded twice on the same sample, and data recorded for identical pairs of (T<sub>H</sub>,  $\kappa$ ) values co-added prior to data processing. For T<sub>H</sub> = 1.25s,  $\kappa_1 = 20 \mu$ s,  $\kappa_2 = 2.5$  ms,  $\kappa_3 = 5$  ms; for T<sub>H</sub> = 2.5s,  $\kappa_1 = 20 \mu$ s,  $\kappa_2 = 1.0$  ms,  $\kappa_3 = 2.0$  ms; for T<sub>H</sub> = 3.75s,  $\kappa_1 = 20 \mu$ s,  $\kappa_2 = 0.5$  ms,  $\kappa_3 = 1$  ms. The interleaved mode of data collection served to minimize any impact that a loss of free monomer peptide concentration (*ca* 15% after 1152

pressure cycles), caused by formation of pressure-resistant species, could have on the apparent decay constants.

Initial attempts to separate monomeric and oligomeric species by DOSY NMR,<sup>5</sup> taking advantage of the difference in translational diffusion rates of monomeric and oligomeric species were also carried out. However, DOSY NMR is adversely impacted by the strong temperature gradients induced by the solvent compression and decompression associated with the pressure jumping and we find such DOSY measurements to generally be incompatible with rapid pressure jumps.

Spectra were processed using nmrPipe,<sup>6</sup> analyzed either by the programs Sparky<sup>7</sup>, ccpnmr analysis v2.4,<sup>8</sup> or using nmrglue python libraries.<sup>9</sup>

### **Transmission electron microscopy**

TEM images were obtained using a FEI Morgagni microscope, operating at 80 kV. Copper 400 grids with a carbon film (Electron Microscopy Sciences, CF400-CU) were glow-discharged just prior to application of 5  $\mu$ l of 250  $\mu$ M sample (pH 6.2) to the grid surface. After 2 min of adsorption, grids were blotted with filter paper, rinsed with 5  $\mu$ l of Milli-Q water, then stained for 1 min with 5  $\mu$ L of 2.5% uranyl acetate, blotted, and air dried. For attaining images at concentrations lower than the NMR sample concentration, upon removal of the sample from the high-pressure NMR tube, samples were rapidly diluted into Milli-Q water followed by a few seconds of mild vortexing, prior to application on the glow-discharged grid. All sample handling for TEM studies was carried out at room temperature.

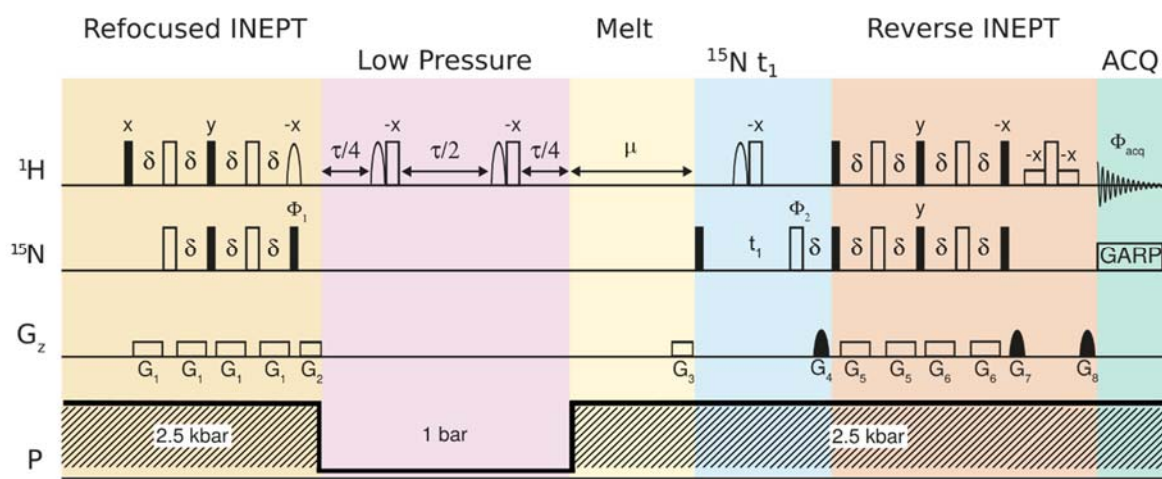


**Figure S1.** Pulse diagram of the  $T_1$ -filtered refocused HSQC experiment for the observation of residue specific rigidification of  $A\beta^{40}$  peptides in the oligomeric state. Initially, following a long (9 s) equilibration period at high pressure, a refocused INEPT sequence is used to generate  $N_{\pm z}$  magnetization (dark yellow shaded region). During the subsequent low-pressure interval (pink) of total duration  $\tau$ , a fraction of monomeric peptide converts to the oligomeric, aggregated state. Inversion of the amide protons at times  $\tau/4$  and  $3\tau/4$  is used to minimize the effect of cross-correlated  $^{15}\text{N}$   $T_1$  relaxation of the monomeric fraction of the sample, where the TROSY component of the  $^{15}\text{N}$  magnetization has an apparent  $T_1$  greater than 1s, adversely impacting the ability to separate monomer and oligomer signals based on their different  $T_1$ . For the oligomeric fraction of the sample, these amide inversion pulses have essentially no effect because their  $^1\text{H}$ - $^1\text{H}$  spin-flip rate is large compared to the spacing between these inversion pulses. The selective  $^1\text{H}$   $180^\circ$  pulses are used to keep the  $\text{H}_2\text{O}$  magnetization along the  $+z$  axis to prevent radiation damping effects. When  $\tau$  is set to 200 ms (i.e.  $< \sim 600$  ms  $^{15}\text{N}$   $T_1$  of monomeric peptide),  $>70\%$  of the initially generated monomeric  $N_{\pm z}$  magnetization will remain present at the end of the low-pressure period. However, for  $\tau = 5.5$  s or 8 s, only magnetization from monomers that oligomerized (which imparts an elongated  $T_1$ ) remains at the end of the low-pressure period. A maximum of only two interleaved 2D spectra with different, long  $\tau$  values could be recorded before formation of pressure-resistant species took over, making it difficult to obtain a more detailed characterization of the  $T_1$  relaxation process. Recording of the short  $\tau$  ( $\tau = 200$  ms) spectrum is of much higher sensitivity and this data set therefore was recorded separately, with scaling of intensities relative to the long  $\tau$  values based on just the first FID of a separate set where only the first FID was retained and all three  $\tau$  values were interleaved. Following a switch back to high pressure and a subsequent “melting period” (light yellow) of duration  $\mu$  (empirically optimized at 350 ms), during which the oligomerized peptide converts back to its disordered, monomeric state, signals are read out using the standard gradient-enhanced HSQC scheme.<sup>10</sup> The duration of  $\mu$  was decremented when  $t_1$  was incremented from 0 to 40 ms, such that the time between the switch from low to high pressure and the start of  $^1\text{H}$  data acquisition remains constant, a detail that serves to eliminate the time-dependence of the effects (e.g. temperature and vibrations) of the pressure jump on the detected  $^1\text{H}$  signals.<sup>4</sup> Filled and open symbols on the  $^1\text{H}$  and  $^{15}\text{N}$  radiofrequency channels represent  $90^\circ$  and  $180^\circ$  pulses, respectively. Shaped pulses are selectively applied to the water resonance, as are the weak rectangular  $90^\circ$  pulses that are part of the standard WATERGATE<sup>11</sup> element. Unless indicated, pulse phases are x. Composite-pulse decoupling on the  $^{15}\text{N}$  channel was used during  $t_2$  acquisition using a GARP-scheme. The INEPT delays,

$\delta$ , were 2.7 ms. Phase cycling:  $\phi_1 = \{y, -y\}$ ,  $\phi_2 = \{x, x, y, y, -x, -x, -y, -y\}$ ,  $\phi_{acq} = \{x, -x, -x, x\}$ . Pulsed field gradients are either sine-bell shaped (G4, 7, 8), or weak rectangular (G1, 2, 3, 5, 6). Gradient durations and peak amplitudes are as follows: G1, 2.6 ms, 0.95 G/cm; G2, 2.0 ms, 8.25 G/cm; G3, 1.0 ms, 3.30 G/cm; G4, 2.0 ms, 15.69 G/cm; G5, 2.6 ms, 0.38 G/cm; G6, 2.6 ms, 0.29 G/cm; G7, 0.5 ms, 9.54 G/cm; G8, 0.5 ms, 15.90 G/cm.

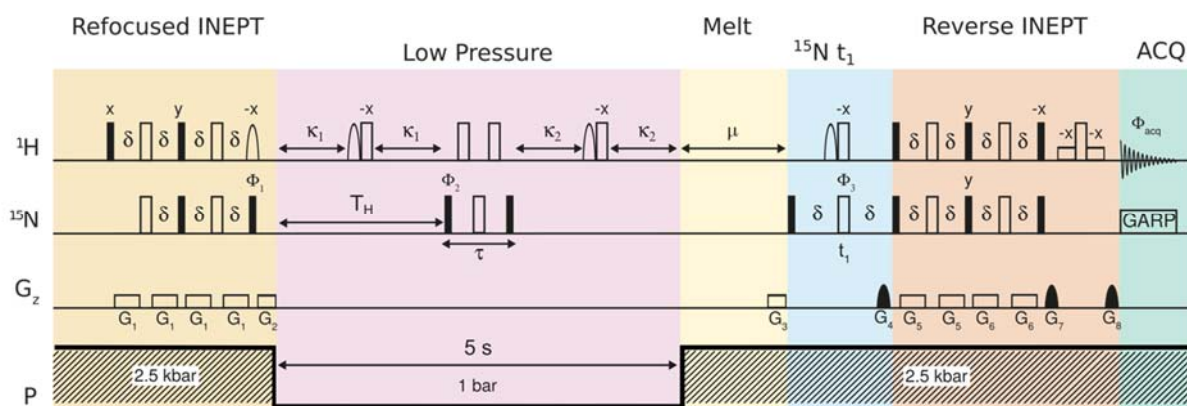


**Figure S2.** Pulse diagram for the observation of transverse relaxation rate of  $A\beta^{40}$  peptides in the oligomeric state, using a  $T_1$ -filtered Hahn-echo  $T_2$  experiment. The pulse sequence is fully analogous to that of Figure S1, but only a 1D spectrum is acquired for  $t_1 = 0$ , and a Hahn-echo block is inserted at time  $T_H$  after the drop to low pressure. Delays  $\kappa_1$  and  $\kappa_2$  are varied such that the  $180^\circ(\text{water})\text{-}180^\circ$  pulse pairs are centered within their respective delay intervals as the Hahn-echo block is moved across the 5-s  $T_1$  filter. Gradients are as in Figure 1S. Phase cycling:  $\phi_1 = \{y, -y\}$ ,  $\phi_2 = \{x, x, -x, -x\}$ ,  $\phi_3 = \{x, x, x, x, y, y, y, -x, -x, -x, -x, -y, -y, -y, -y\}$ ,  $\phi_{acq} = \{x, -x, -x, x, -x, x, x, -x\}$ .

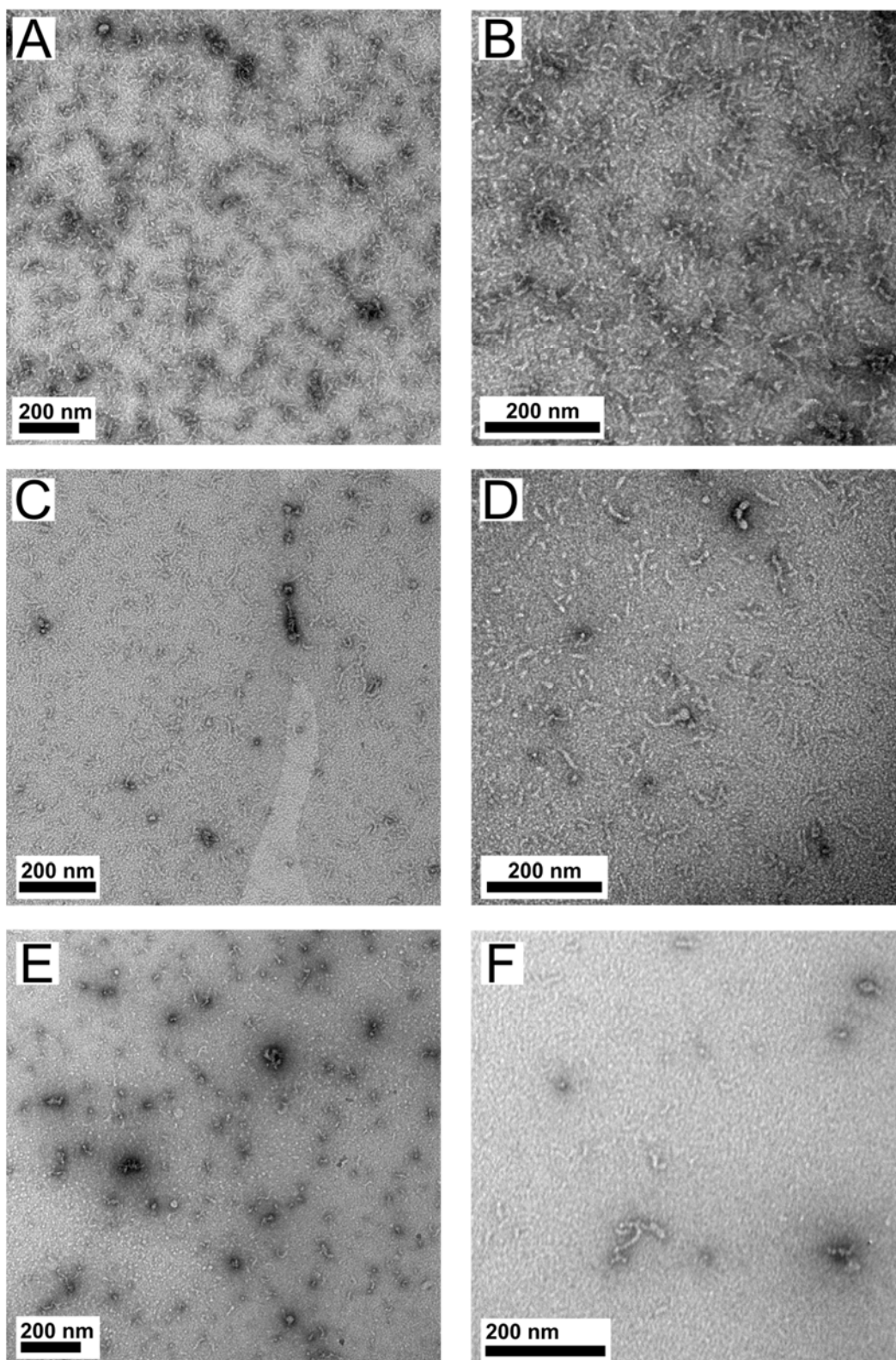


**Figure S3.** Negatively stained TEM images of a fresh A $\beta^{40}$  sample at 250  $\mu$ M (A, B), 50  $\mu$ M (B, C), and 25  $\mu$ M (E, F) dilutions, where lower concentrations were diluted into Milli-Q water. The samples were applied to EM grids at *ca.* 90 seconds post pressure-drop from 2.5 kbar to 1 bar. Small, lightly staining, worm-shaped oligomers/protofibrils are observed at all concentrations, with additional darkly staining aggregates also present. The latter tend to become more pronounced for longer delays between the pressure drop and dispersing the sample on the grid.

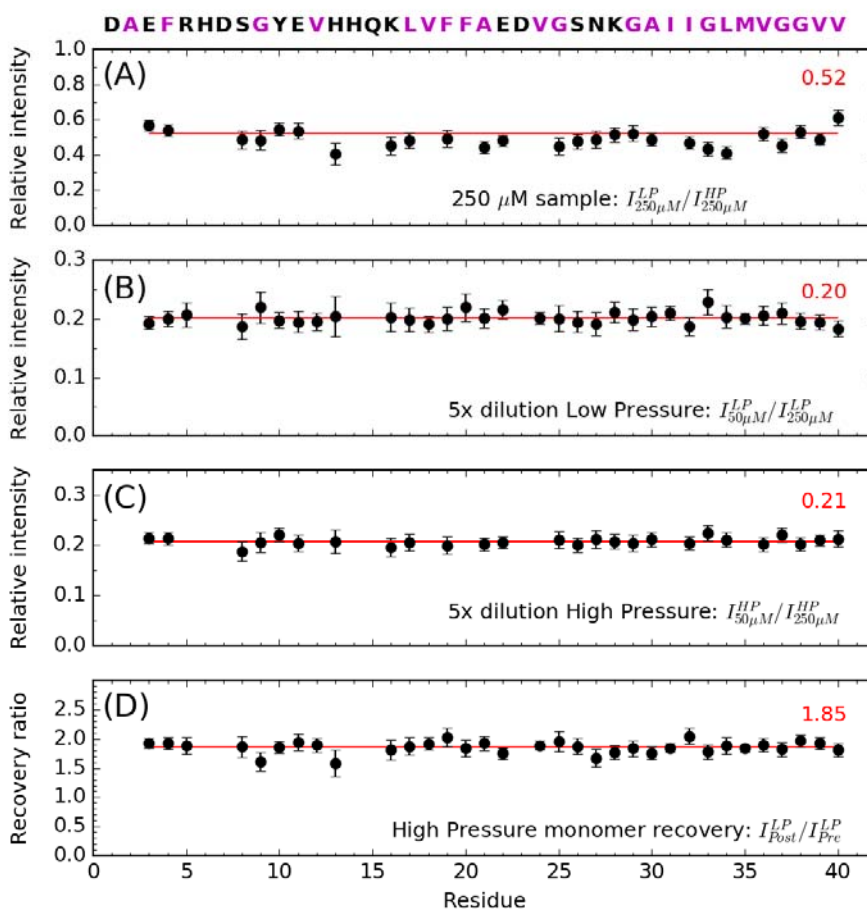


**Figure S4.** Spectral intensity ratios as a function of residue number to investigate solubility of oligomers, initially prepared at 1 bar, 250  $\mu\text{M}$   $\text{A}\beta^{40}$ , in the same manner as the more concentrated samples used for the  $T_1$  and  $T_2$  measurements. Average values of the intensity ratios are marked by the red horizontal lines, with numerical values indicated at the top right of each panel. Intensities were scaled for the number of transients per FID, prior to calculating the ratios. (A) Ratio of intensities of 5-minute HSQC spectra (2 transients per FID, 20  $^\circ\text{C}$ .) recorded after dropping the pressure to 1 bar,  $I_{250\mu\text{M}}^{\text{LP}}$ , and the corresponding spectrum taken immediately prior to that, at 2.5 kbar,  $I_{250\mu\text{M}}^{\text{HP}}$ . To account for the *ca* 8% volume compression of the solvent at 2.5 kbar relative to 1 bar, the  $I_{250\mu\text{M}}^{\text{HP}}$  intensities were scaled by 0.92 prior to calculating the ratio. (B) HSQC (32 transients, 75 minutes) intensity ratios of the five-fold diluted sample at 1 bar,  $I_{50\mu\text{M}}^{\text{LP}}$ , over the sample containing 250  $\mu\text{M}$   $\text{A}\beta^{40}$  at 1 bar,  $I_{250\mu\text{M}}^{\text{LP}}$ . The observation that the intensities scale by the dilution factor indicates that the oligomers have not converted back to observable monomers. (C) HSQC intensity ratios of the five-fold diluted sample, recorded at 2.5 kbar,  $I_{50\mu\text{M}}^{\text{HP}}$  and the original 250  $\mu\text{M}$  sample,  $I_{250\mu\text{M}}^{\text{HP}}$ , confirming that the dilution factor is accurate. (D) HSQC intensity increase,  $I_{50\mu\text{M}}^{\text{LP,Post}} / I_{50\mu\text{M}}^{\text{LP,Pre}}$  obtained by resolubilizing the oligomers of the diluted sample, with solubilization obtained by temporarily increasing the pressure to 2.5 kbar (for 75 minutes, to record the  $I_{50\mu\text{M}}^{\text{HP}}$  intensities, used for (C)).  $I_{50\mu\text{M}}^{\text{LP,Pre}}$  intensities correspond to  $I_{50\mu\text{M}}^{\text{LP}}$  values used for generating panel (B).

## References

1. Peterson, R. W.; Wand, A. J., Self-contained high-pressure cell, apparatus, and procedure for the preparation of encapsulated proteins dissolved in low viscosity fluids for nuclear magnetic resonance spectroscopy. *Rev. Sci. Instrum.* **2005**, *76* (9).
2. Quinlan, R. J.; Reinhart, G. D., Baroresistant buffer mixtures for biochemical analyses. *Anal. Biochem.* **2005**, *341* (1), 69-76.
3. Ying, J.; Barnes, C. A.; Louis, J. M.; Bax, A., Importance of time-ordered non-uniform sampling of multi-dimensional NMR spectra of Abeta1-42 peptide under aggregating conditions *J. Biomol. NMR.* **2019**, doi: 10.1007/s10858-019-00235-7
4. Charlier, C.; Alderson, T. R.; Courtney, J. M.; Ying, J.; Anfinrud, P.; Bax, A., Study of protein folding under native conditions by rapidly switching the hydrostatic pressure inside an NMR sample cell. *Proc. Natl. Acad. Sci. USA* **2018**, *115*, 201803642.
5. Morris, K. F.; Johnson, C. S., Diffusion-ordered two-dimensional nuclear magnetic resonance spectroscopy. *J. Am. Chem. Soc.* **1992**, *114*, 3139-3141.
6. Delaglio, F.; Grzesiek, S.; Vuister, G. W.; Zhu, G.; Pfeifer, J.; Bax, A., NMRpipe - a multidimensional spectral processing system based on Unix pipes. *J. Biomol. NMR* **1995**, *6* (3), 277-293.
7. Lee, W.; Tonelli, M.; Markley, J. L., NMRFAM-SPARKY: enhanced software for biomolecular NMR spectroscopy. *Bioinformatics (Oxford, England)* **2015**, *31*, 1325-7.
8. Skinner, S. P.; Fogh, R. H.; Boucher, W.; Ragan, T. J.; Mureddu, L. G.; Vuister, G. W., CcpNmr AnalysisAssign: a flexible platform for integrated NMR analysis. *J. Biomol. NMR* **2016**, *66* (2), 111-124.
9. Helmus, J. J.; Jaroniec, C. P., Nmrglue: an open source Python package for the analysis of multidimensional NMR data. *J. Biomol. NMR* **2013**, *55*, 355-367.
10. Kay, L. E.; Keifer, P.; Saarinen, T., Pure Absorption Gradient Enhanced Heteronuclear Single Quantum Correlation Spectroscopy with Improved Sensitivity. *J. Am. Chem. Soc.* **1992**, *114*, 10663-10665.
11. Piotto, M.; Saudek, V.; Sklenár, V., Gradient-tailored excitation for single-quantum NMR spectroscopy of aqueous solutions. *J. Biomol. NMR* **1992**, *2* (6), 661-665.